KKU Engineering Journal

http://www.en.kku.ac.th/enjournal/th/

Airflow simulation using computational fluid dynamics in a complex terrain: the consideration of wind speed, turbulent intensity and inflow angle

Akraphon Janon* and Panumas Srinor

Department of Mechanical Engineering, Faculty of Engineering, Khon Kaen University, Khon kaen, Thailand,40002.

Received October 2013

Accepted December 2013

Abstract

This paper presents an investigation of airflow over a rugged mountain to find suitable locations for wind turbines. The investigation considers turbulent intensity and inflow angle in addition to wind speed. The area of interest is the mountain around the upper reservoir of Lamtakong Jolabha Vadhana Hydro Power Plant, Nakhon Ratchasima, Thailand. The Lamtakong Wind Turbine Power System is located near the reservoir. Due to the ruggedness of the site, according to the angle of slopes, the existing turbines may be experiencing airflow with high turbulent intensity and non-zero inflow angle. This study uses Computational Fluid Dynamics (CFD) and Wind Atlas Analysis and Application Program (WAsP) to simulate airflow. CFD is used in the final analysis to quantify turbulent intensity and inflow angle. The turbulence model is used, while the roughness height and roughness constant are tuned according to the ground cover. Detailed examinations of cases show that the highest wind speeds do not always occur at the mountain's peaks. High turbulent intensity leads to the exclusion of locations on the lee side of the mountain, where it reaches 18%. The inflow angles are high on the upwind side of the mountain and can go up to 20 degrees. It is found that the slopes affect the inflow angles but they do not dictate the inflow angles. Finally, the results of the highest peak suggest that most suitable turbine spot is approximately 60 m downwind from the point of highest wind speed. The power density reduces from 515.3 W/m2 to 502.6 W/m2 at 60 m hub-height. Thus, to achieve a zero inflow angle, turbines may have a power output reduction but they will experience lower turbulence and uneven loading.

Keywords: Inflow angle, Turbulent intensity, CFD, Complex terrain

*Corresponding author

Email Address: Akraphon@kku.ac.th

1. Introduction

Global energy consumption has been rising at an alarming rate. Most sources of energy people consume are fossil fuels, which are finite sources. To sustain our activities, engineers need to raise energy consumption efficiency while improving renewable energy technologies. The interest in renewable energy sources is high. Wind energy is a renewable energy source, which has been utilized for centuries in grain milling, water pumping and sailing. The commonly used technique is electricity production from wind using wind turbines. Wind energy resources differ from location to location. They depend on factors such as geography, season and vegetation. To harvest energy from wind effectively, wind turbines need to be installed at locations where the wind speeds are high and consistent. One of the difficulties in harvesting wind energy is finding the most productive location for wind turbines. The long-term investment nature of wind farm projects necessitates the viable decision at the start.

A macro scale wind map is required to identify potential locations for wind turbine installation. During this process, several areas with high wind speeds or wind power per unit area can be found. After that, a wind speed measuring program has to be conducted in those areas. A very detailed wind map specific to the area is made using the measured data and simulation. Studies have been done in the North and South of Thailand to identify locations with viable wind resources [1,2]. Measured data and Wind Atlas Analysis and Application Program (WAsP) were used to produce detailed wind maps: micro scale wind maps. WAsP is used worldwide in wind resource assessment. However, the operating envelope of WAsP is within analysis of areas where the terrain slopes are less than 17 degrees [3]. Such terrain ensures the airflow is an attached flow. Slopes that are greater will generate separated flow, which renders WAsP unreliable [4]. This is due to the fact that WAsP is a program using a linear modeling approach. Researchers have turned to a non-linear modeling approach using Computational Fluid Dynamics (CFD) to avoid such problems.

Comparisons between modeling for wind resource using WAsP and CFD software in complex terrains have shown that CFD software gives more accurate results [5-7]. CFD software uses computational power to solve the Navier-Stokes equations, which express the principles of conservation of momentum, mass and energy. By solving these equations, energy dissipated in the form of turbulence can be represented. Turbulence is of the primary interest because we are interested in the flow within the boundary layers. The flow in this region is turbulent. Alan Russell [8] used the $k-\varepsilon$ turbulence model in CFD software to simulate airflow over Cinder Cone Butte (Idaho, USA). The predicted wind speeds were 23% higher than those obtained using WAsP. However, the study did not report turbulent intensity, which would be necessary for a wind turbine installation consideration. Apart from the $k-\varepsilon$ turbulence model, there are other flow models solvable within the CFD environment such as Renormalisation Group (RNG), Reynolds Averaged Navier-Stokes (RANS) and other proprietary models. In addition, simulations must be validated against measured data. Teerapong Boonterm [9] investigated airflow over a rugged terrain to find potential causes of aircraft accidents at an army airport. Various turbulence models were used to analyse airflow over the airport. The

measured wind speed data was used to validate the results. Even though turbulent intensity should have been the focus of this investigation as one of the potential causes, it was not mentioned in the study.

Turbulence has negative effects on wind turbines because it creates uneven loading. Firstly, an ideal flow would have instantaneous wind speeds fluctuating around an average wind speed. As the flow becomes more turbulent, the fluctuation increases. Large wind speed fluctuation causes fatigue on turbine blades [10]. Secondly, the kinetic energy in the wind dissipates as the mass of air mixes. Thus, the energy in the wind is reduced. In addition, the flow direction is changed by the formation of vertexes and then the inflow angle of air into the wind turbines is altered. It reduces the effectiveness of the airfoils. Non-zero inflow angle can be seen in locations with rugged terrain. The recommended maximum inflow angle is 8 degrees [11]. Because the non-zero inflow angle is a local phenomenon, CFD is required to visualise it. The solution is to place wind turbines at a distance away from turbulence sources or increase the hub height [3, 10, 12].

Turbulent intensity and inflow angle are examined in addition to wind speed in an investigation to find the most productive wind turbine locations in a rugged terrain. The inclusion of turbulent intensity and inlet flow angle will help us choose wind turbine locations to ensure low vibration and uneven loading on turbines. CFD (ANSYS 14.0) and WAsP 10.0 are used to analyse airflow over a mountainous area where the slopes are higher than 17 degrees (rugged terrain). A mountain in the Northeast of Thailand was chosen as a case study.

2. Materials and methods

2.1 Investigated site

Airflow over a mountain is investigated around the upper reservoir of the Lamtakong Jolabha Vadhana Hydro Power Plant, Nakhon Ratchasima, Thailand. The Lamtakong Wind Turbine Power System is located nearby. We consider airflow to come in at 270 degrees (West) of the top of the mountain. The wind speeds at 60 m above ground level (agl) are considered because 60 m is the common hub-height of turbines and other wind monitoring projects. The area is rugged and approximately 650 m above sea level (asl). A height contour map of the area is made into a 6x6 km^2 size. The ruggedness of the terrain is quantified by calculating the angle of slopes. Slopes that are steeper than 17 degrees are shown in a dark colour (figure 1). Airflow is simulated over the mountain but results of analysis along 3 lines (A, AA and AAA) are shown as examples. The line AA passes through the Lamtakong Wind Turbine Power System, which is owned by the Electricity Generating Authority of Thailand (EGAT).

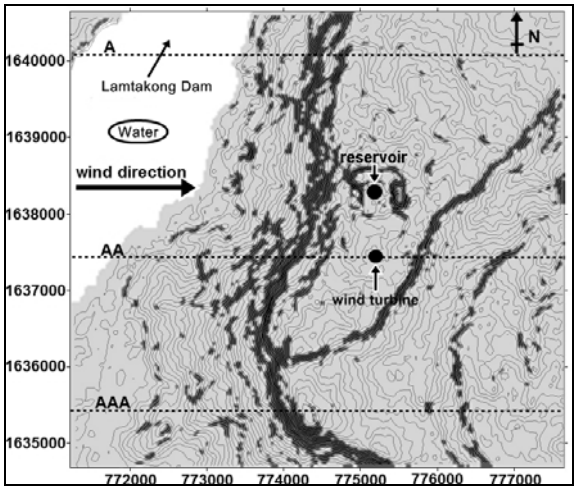

Figure 1 The height contour map of the area around the upper reservoir of the Lamtakong Jolabha Vadhana Hydro Power Plant. The highest point is 650 m above sea level and there is a body of water on the left. The dark colour illustrates locations with slopes steeper than 17 degrees

2.2 Analytical equations

Nomenclature

u,V	velocity (m s^{-1})	Re	Reynolds number
ρ	density (kg m^{-3})	D_H	hydraulic diameter
p	pressure (Pa)	μ	viscosity (kg$m^{-1}s^{-1}$)
		g	gravity component

A	cross-sectional area
z_0	surface roughness (m)
z	height above the surface (m)
κ	Karman's constant (=0.41)
I	turbulence intensity
μ_t	turbulent viscosity (kg $m^{-1}s^{-1}$)
ε	turbulent dissipation rate (m^2s^{-3})
k	turbulent kinetic energy (m^2s^{-2})
x	cartesian coordinates
u_*	frictional velocity (m s^{-1})

The airflow is governed by three principles: the conservation of mass, momentum and energy. The conservation of mass is stated by the continuity equation (1). A mass of moving air exchanges momentum with the surrounding air and objects and the change in momentum is stated by the momentum equation (2).

Continuity Equation

$$\frac{\partial \rho}{\partial t}+\frac{\partial(\rho\overline{u_i})}{\partial x_i}=0 \qquad (1)$$

Momentum Equation

$$\frac{\partial \rho(\overline{u_i}\,\overline{u_j})}{\partial x_i}= -\rho\delta_{ij}g-\frac{\partial \overline{p}}{\partial x_i}+\frac{\partial}{\partial x_j}\left[\mu\frac{\partial \overline{u_i}}{\partial x_j}\right]-\frac{\partial(\overline{\rho u_i' u_j'})}{\partial x_j}\frac{n!}{r!(n-r)!} \qquad (2)$$

$k-\varepsilon$ model is used in the turbulence study because it is quick and accurate. An experiment by Alinot and Masson [13] provides the five constants needed for the analysis. These five constants are $C_{\varepsilon 1}$ =1.176, $C_{\varepsilon 2}$ =1.92, C_{μ} =0.03329, σ_k ,=1.0 and σ_{ε} =1.3. Turbulent kinetic energy (k), or kinetic energy per unit mass can be computed by using equation 3. This kinetic energy is dissipated due to friction and mixing action. The rate of kinetic energy dissipation is governed by equation 4.

$$\frac{\partial\left(\rho k\overline{u_i}\right)}{\partial x_i}= \frac{\partial}{\partial x_j}\left[\left(\mu+\frac{\mu_t}{\sigma_k}\right)\frac{\partial k}{\partial x_j}\right]-\overline{\rho u_i' u_j'}\frac{\partial \overline{u_j}}{\partial x_i}-\rho\varepsilon \qquad (3)$$

$$\frac{\partial\left(\rho\varepsilon\overline{u_i}\right)}{\partial x_j}= \frac{\partial}{\partial x_j}\left[\left(\mu+\frac{\mu_t}{\sigma_\varepsilon}\right)\frac{\partial \varepsilon}{\partial x_j}\right]-C_{\varepsilon 1}\left(\frac{\varepsilon}{k}\right)\overline{\rho u_i' u_j'}\frac{\partial \overline{u_j}}{\partial x_i}-C_{\varepsilon 2}\rho\frac{\varepsilon^2}{k} \qquad (4)$$

There are three groups of equations, which are turbulent viscosity, wall function and turbulent intensity equations. The turbulent viscosity equation (equation 5) gives the numerical relationship between k and ε through turbulent viscosity (μ_t). The wall function equations (equations 6, 7 and 8)

enable us to numerically compute the fluid shear stress as a function of velocity at a given distance from the wall. The logarithmic relationship (equation 6) is sometimes called Log Law of The Wall [14]. Finally, the inlet turbulent intensity equations (9, 10 and 11) are used to set up the flow conditions in a fully developed flow.

$$\mu_t = \rho^* C_\mu \frac{k^2}{\varepsilon} \quad (5)$$

$$U = \frac{u_*}{\kappa} \ln \frac{z}{z_0} \quad (6)$$

$$k = \frac{u_*^2}{C_\mu^{1/2}} \quad (7)$$

$$\varepsilon = \frac{u_*^3}{kz} \quad (8)$$

$$I = 0.16(\mathrm{Re}_{D_H})^{(-1/8)} \quad (9)$$

$$\mathrm{Re}_{D_H} = \frac{\rho V D_H}{\mu} \quad (10)$$

$$D_H = \frac{4A}{P} \quad (11)$$

Table1 Roughness heights and roughness constants dictate the levels of friction. The values used are modified in this study.

Model Parameter	ANSYS Default	Pattanapol et al. [15]
Roughness Height (z)	0.05m	1.5m
Roughness Constant	0.5	0.327

The roughness height (z) and roughness constant characterise the friction force produced by a surface. These numbers depend on the sizes, heights and spacing between obstacles on the ground. The numbers are usually selected by a visual inspection of the vegetation. The default values in ANSYS 14.0 are 0.05 m and 0.5, respectively. They are suitable for simulation of flow problems in pipes and therefore must be changed. The numbers investigated by Pattanapol et al. are used [15] (Table 1).

2.3 Simulation model set up

A digital contour map is obtained and then an enclosing volume on top of the map is built. The volume is 6000x6000x1000 m (WxLxH) in dimensions (Figure 2). The upper reservoir of the Lamtakong Jolabha Vadhana Hydro Power Plant is in the middle of the map and air flows from West to East (left to right). The boundary conditions are assigned as follow;

- The air flows into the map where the wall (left) is assigned as Velocity Inlet.
- The air flows out of the map where the wall (right) is assigned as Outflow.
- The walls along the sides and the ceiling are assigned to be Symmetry, which means they are not physical walls. Therefore, they do not exert any force onto the moving fluid.

The ground is assigned as a wall with a uniform roughness height and roughness constant (table 1).

2.4 Grid independent testing

The entire volume is divided by a meshing process into smaller volumes called elements. The greater the numbers of elements the more accurate the solutions will be. However, solving a problem using large numbers of elements consumes more computing resources and time. Therefore, an appropriate number of elements must be specified to use less computing resources while achieving accurate results.

This is achieved by varying the surface grid sizes at 30, 40, 50 and 70 (Table 2) and then simulating for solutions. The smaller grid size results in large numbers of elements. We further improve the meshing process by assigning smaller grid sizes to locations with complex geometry to increase local accuracy and using large grid sizes elsewhere to reduce computing resources and time.

Table 2 The smaller surface grid size results in large numbers of elements. Using smaller grid size will increase the computing time needed

Surface Grid Size (m)	*30*	*40*	*50*	*70*
Number of Elements	847400	442740	301940	153060

At each case of the surface grid size, wind velocities along the AA line are compared. A graph between distance (from inlet to outlet) and velocity is plotted to show the difference between cases (figure 3). It is found that the surface grid size of 40 m gives wind velocities within 5% of that of the 30 m. However, the number of elements is approximately halved, so it uses less resources and time. Therefore, the grid size of 40 m is used throughout. After the setup is identified, we simulate airflow over the mountain by varying the inlet wind speeds at 2, 3, 4 and 5 m/s.

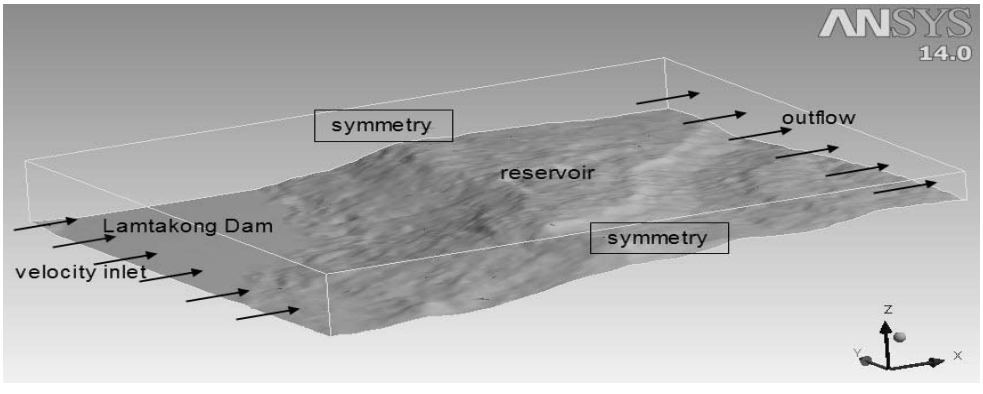

Figure 2 3D surface map is enclosed by an imaginary volume to signify calculation envelope

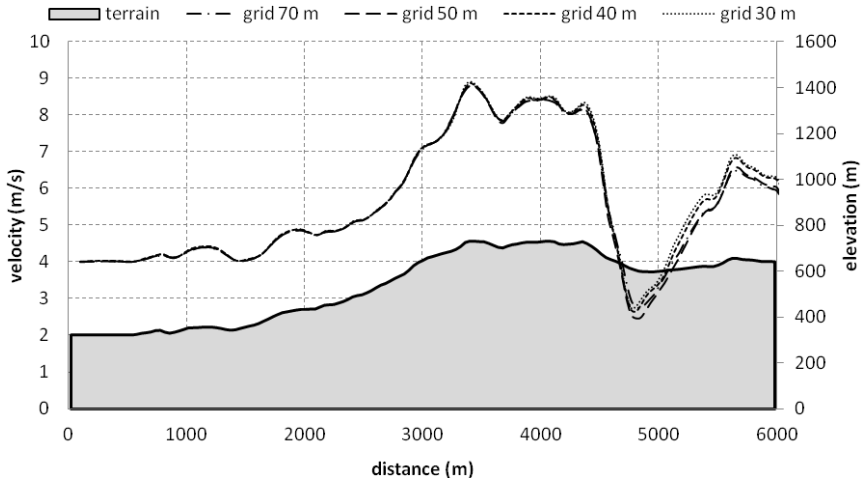

Figure 3 Wind velocities along the line AA when different surface grid sizes are used

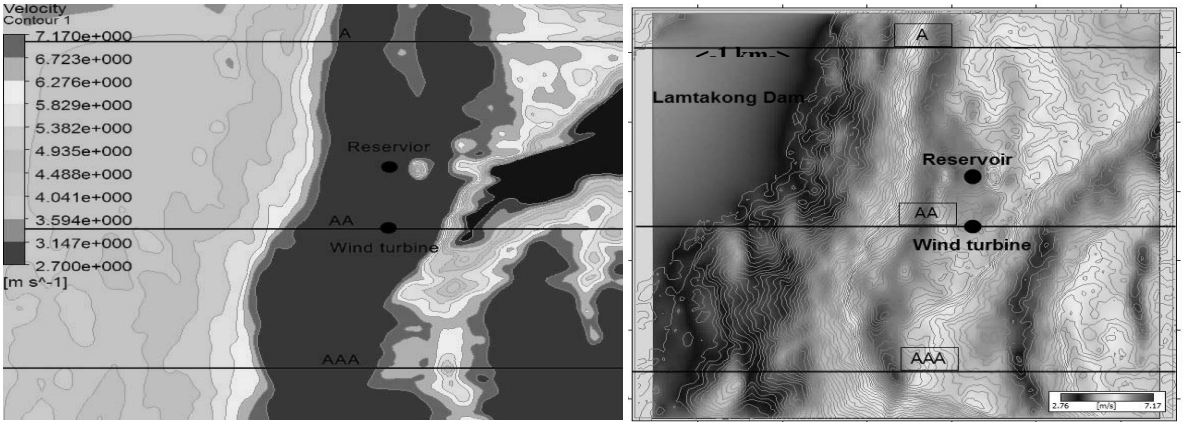

(a) (b)

Figure 4 (a) A velocity gradient plot of results from a simulation using CFD when the inlet air velocity is 4 m/s. (b) A velocity gradient plot of results from a simulation using WAsP when the inlet air velocity is 4 m/s. The gradient scale is 2.7-7.17 m/s on both plots

2.5 WAsP modelling

A digital elevation model is produced with 10 m height contour. A Roughness of the surface can be specified by drawing areas, where each area has uniform vegetation to give a uniform roughness. However, a uniform roughness is specified for the entire map for consistency. The values used are the same for CFD. The wind rose, where the wind speeds and directions are the same for CFD, is input into the program. The resultant wind map is obtained.

3. Results and discussion

3.1 Wind speed comparison between CFD (ANSYS 14.0) and WAsP 10.0

The results of simulations from CFD and WAsP are plotted in the form of velocity gradient maps. The wind speeds are represented in colours scale from 2.7-7.17 m/s. Wind speeds obtained from a simulation using CFD when the inlet wind speed is 4 m/s are shown in figure 4a. According to figure 4a, the airflow speeds up as the elevation increases. There are areas where wind speed increases more than that of the inlet along the mountain top and then the wind speeds drop below
the inlet value as air flows pass the reservoir. Although the results from a simulation using WAsP illustrate similar trends (Figure 4b), there are a few differences. Firstly, the magnitudes of wind speeds at the mountain top are approximately 30% lower. Secondly, the areas of the highest and lowest wind speeds are different.

Furthermore, CFD is capable of showing the turbulent intensity. Turbulent intensity is plotted in a gradient plot (Figure 5). The results show turbulent intensity is under the threshold in areas between the water and the cliff face of the mountain. The turbulence increases as air flows over the mountain (2-6%) and then increases on the lee side of the mountain (12-18%). The threshold of turbulent intensity is 18% [15].

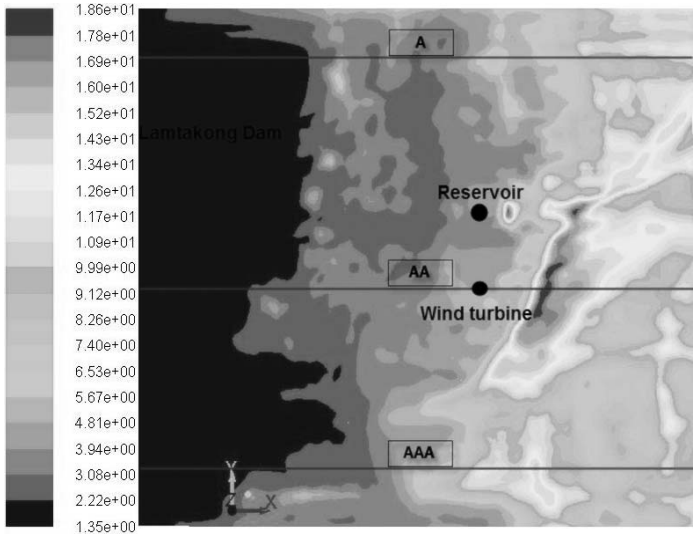

Figure 5 Turbulent intensity plot obtained using CFD. The plot visually identifies locations with turbulent intensity values. The red colored areas have higher turbulent intensities

3.2 Turbulent Intensity and Inflow angle consideration

Airflow over the mountain is simulated using both WAsP and CFD for comparison purposes but only results from CFD simulations will be considered here. The abilities of showing wind speed, turbulent intensity and inflow angles of CFD will help us to identify areas which fit the criteria for wind turbine installation. For illustration purposes, the results along 3 chosen lines (A, AA and AAA) will be investigated. The elevation, speed-up ratio, turbulent intensity, inflow angle and slope angle are plotted against the distance from the inlet to outlet. The speed-up ratio is the ratio between the increase of instantaneous wind speed over the inlet wind speed. The results show that the inflow angles range from 2 to 7 degrees for all cases. To be able to efficiently utilise the energy in the airflow and reduce fatigue load on turbine blades, the recommended turbine locations along the 3 lines need to be moved.

Along the line A (Table 3), the spot with the highest speed-up ratio is at 3689 m from the inlet and has power density of 359.7 W/m^2 at 60 m hub-height. The turbine needs to be moved to 3733 m, where the inflow angle is zero. The power density reduces to 351.8 W/m^2, while the turbulent intensity is under the threshold. Moreover, the EGAT wind turbines on the line AA (Table 4) are not at the position of the highest speed-up ratio. However, their positions perform close to our recommended position in regard to inflow angle, power density and turbulent intensity. Along the line AAA (Table 5), the highest speed-up ratio occurs at 2979 m where the power density is 515.3 W/m^2. Our recommended spot is at 3040 m where the inflow angle reduces from 7 to 0 degrees. The power density reduces to 502.6 W/m^2. The move of the position may reduce power density but turbines will experience less vibration and uneven loading.

It is evident that the inflow angles on the upwind side are generally greater and should be avoided. However, the turbulent intensity is the highest on the lee side (Figures 6a and 6b). Therefore, It concludes that wind turbines should not be installed at a distance far into the upwind and lee sides of the mountain. Thus, areas around the top of the mountain are the most suitable in regard to turbulent intensity.

Then, turbine locations can be fine-tuned by considering the speed-up ratio, inflow angle. It must be noted that the highest speed-up ratios or wind speeds do not necessarily occur at the peak of the mountain. In addition, the inflow angle is not zero at that point (Figures 7a and 7b). A zero inflow angle can sometimes be found in a spot that is not flat. Therefore, wind turbine installation at the peaks may not always yield the highest energy production, while relying on the spots with the highest wind speeds will increase the vibration and uneven loading of turbines.

4. Conclusions

From our investigation of airflow over a rugged mountain, locations with the highest power densities for wind turbine installation are found. The criteria used in the investigation are wind speed, turbulent intensity and inflow angle. These parameters are employed to guard against the perception that high energy yield spot for a wind turbine is likely to be at the peak of a mountain.

Upon a closer inspection, the highest wind speed can occur away from the peak of the mountain.

Turbulent intensities closer to the threshold are found on the lee side of the mountain, which should be avoided in regard to wind turbine installation. High turbulent intensity reduces the efficiency of the airfoils and accelerates fatigue wear on turbines. High turbulence also coincides with a drop in wind speed because the kinetic energy in the moving air is dissipated in the phenomenon. The orography of a mountain causes inflow angles to change. But inflow angles do not necessarily follow the slopes of a mountain. Although inflow angles close to zero can be found near the top of a mountain, a close inspection is required to fine-tune for a zero inflow angle position.

Table 3 Details of results along the line A when the inlet velocity is 4 m/s. The recommended turbine position (*) is dictated by the inflow angle

Distance (m)	2011	2520	2997	3521	3689	3733*	4013	4488
Velocity (m/s)	4.1	4.4	4.8	7.8	8.3	8.3	7.0	7.7
Power density (w/m^2)	44.6	51.6	63.6	279.7	359.7	351.8	215.6	276.5
Inflow angle (deg)	1.0	9.7	11.8	11.8	2.0	0.0	-2.7	-1.3
Turbulent Intensity (%)	2.3	3.7	4.3	1.8	1.7	1.8	3.3	3.1

Table 4 Details of results along line AA when the inlet velocity is 4 m/s. At the distances of 3490 (EGAT wind turbines), the inflow angle is zero

Distance (m)	*2019*	*2490*	*2992*	*3394**	*3490*	*3997*	*4070*	*4488*
Velocity (m/s)	4.8	5.1	7.1	8.9	8.7	8.4	8.5	7.2
Power density (w/m^2)	66.1	79.3	207.0	419.5	389.3	365.8	373.4	225.6
Inflow angle (deg)	3.6	9.1	11.7	4.6	0.0	0.5	-0.7	-5.8
Turbulent Intensity (%)	2.6	3.1	1.9	1.8	1.9	2.3	2.2	6.0

Table 5 Details of results along line AAA when the inlet velocity is 4 m/s

Distance (m)	*2000*	*2514*	*2979*	*3040**	*3513*	*4003*	*4520*
Velocity (m/s)	4.9	5.7	9.5	9.4	8.0	7.0	6.2
Power density (w/m^2)	68.2	108.6	515.3	502.6	306.5	209.2	146.2
Inflow angle (deg)	7.4	11.3	7.0	0.0	-4.8	-2.7	-0.2
Turbulent Intensity (%)	3.1	5.5	1.9	1.8	2.9	5.2	6.9

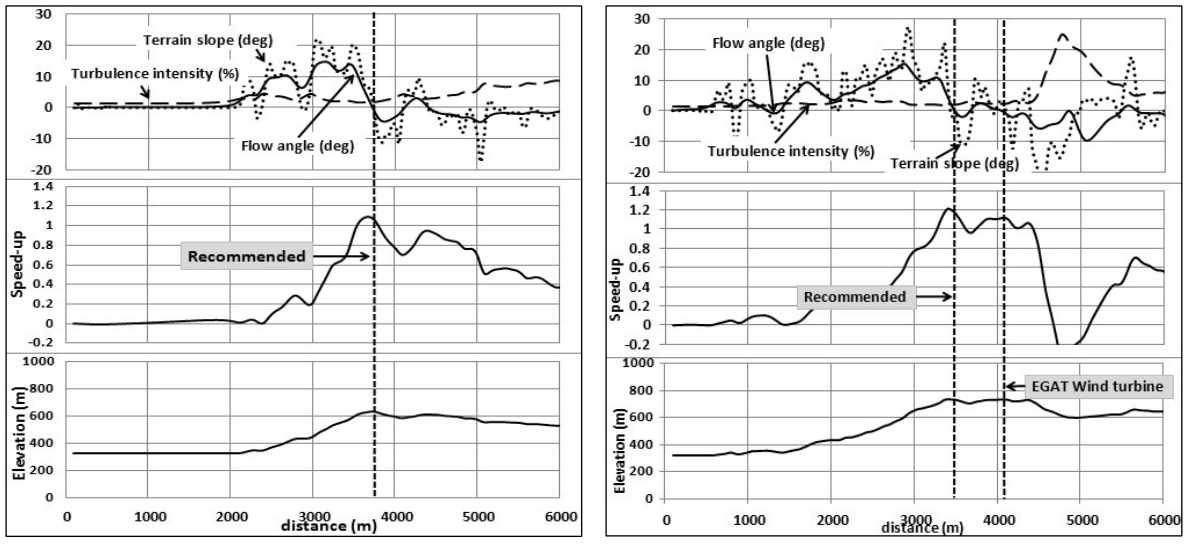

(a) (b)

Figure 6 (a) Plots of paremeters along the line A from inlet to outlet. (b) Plots of paremeters along the line AA

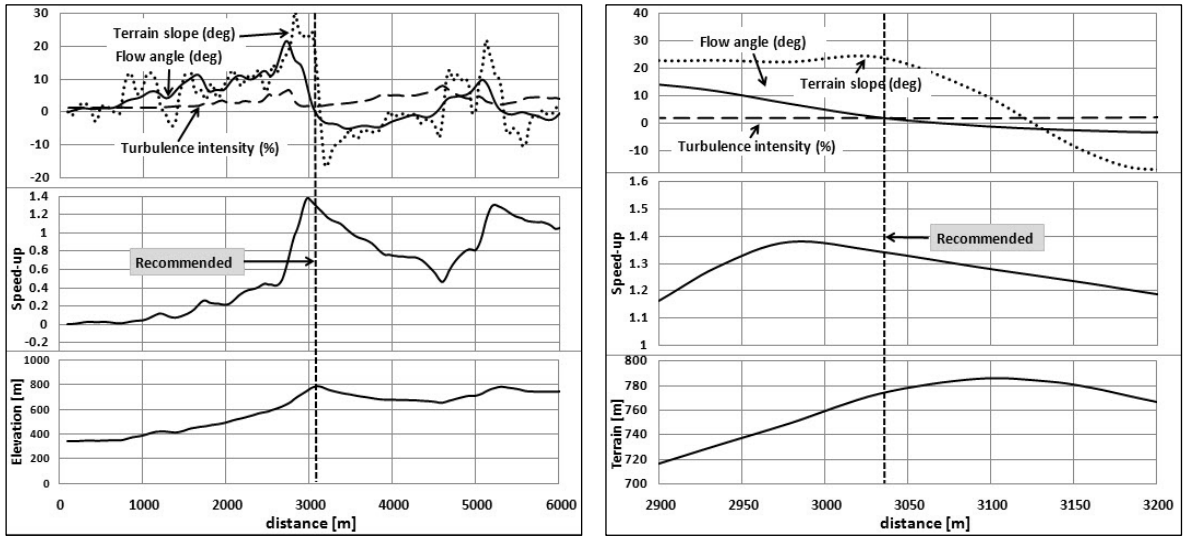

(a) (b)

Figure 7 (a) Plots of parameters along the line AAA. Inflow angles are generally high and reach 20 degrees on the upwind side of the mountain. (b) A close-up of parameters along the line AAA

5. Acknowledgements

The authors would like to thank the Center for Alternative Energy Research and Development, Khon Kaen University, for providing financial support in the form of tuition fees, which enable us to focus on the job at hand.

6. References

[1] Dussade N, Kiatsiriroat T. *Study on Potential of Power Generation from Wind Energy in Upper Northern Region* (Report), Maejo University, Thailand, 2006.

[2] Waewsak J, Kongruang C, Tirawanichakul, S, Tirawanichakul , Matan N. *The feasibility study of wind farm power plants along the coastal lines of southern Thailand* (Report), Thaksin University, Thailand, 2007.

[3] Tong W. *Wind Power Generation and Wind Turbine Design*, p. 78-82, WIT Press, Southampton, UK,2010.

[4] Oke TR. *Boundary Layer Climates*, p. 182-189, University Press, Cambridge,1978.

[5] Mortensen NG, Bowen AJ, Antoniou I. *Improving WAsP predictions in (too) Complex Terrain* (Report), Wind Energy Department, Risø National Laboratory, 2006.

[6] Pereira R, Guedes R, Santos CS. *Comparing WAsP and CFD wind resource estimates for the "regular" user*, Proceedings from EWEC 2010, Warsaw, Polland, 19th April 2010.

[7] Theodoropoulos P. *Validation and Comparison between CFD and Linear WAsP model performance in vertical profile estimation using measurements from a 65m tall mast* (Report), Laboratory of Istos Renewables Ltd, 2008.

[8] Russell A. *Computational Fluid Dynamics Modeling of Atmospheric Flow Applied to Wind Energy Research* (Thesis), Boise State University College of Engineering, USA, 2009.

[9] Boonterm T, Kittichaikarn C. *Analysis and Simulation of Air Flow over Complex Terrain Case Study: Air Flow over Phuka Mountain in Lopburi, Thailand*, ME-NETT 23rd, Chiang Mai, Thailand, 4-7th November 2009.

[10] Frandsen S, Thøgersen M L. Integrated fatigue loading for wind turbines in wind farms by combining ambient turbulence and wakes. *Wind Engineering*, 1999;23: 327-339.

[11] International Electrotechnical Commission *Wind Turbine Generator Systems Part1: Safety Requirements*, International Electro technical Commission, 3rd ed. 2005.

[12] Rodrigo J S, Beeck JV. Dezsoweidinger, G. Wind Tunnel Simulation of the Wind Conditions inside Bi-dimensional Forest Clear-cuts. Application to Wind Turbine Siting, *Journal of Wind Engineering and Industrial Aerodynamics*, 2007;95: 609-634.

[13] Alinot C, Masson C. *Aerodynamic Simulations of Wind Turbines Operating in Atmospheric Boundary Layer with Various Thermal Stratifications*, AIAA-2002-42 ASME Wind Energy Symposium 40th collection of technical papers, Reno, 2002.

[14] Memon, N. *Wind Resource Assessment in Complex Terrain Using CFD* (Thesis), Technical University of Denmark, Denmark. 2005.

[15] Pattanapol W, Wakes S J, Hilton M J. Dickinson K J M. Modeling of Surface Roughness for Flow over a Complex Vegetated Surface, *International Journal of Mathematical, Physical and Engineering Sciences*,2008;2:18-26.